

High Temperature Durability of CFRP Laminated RC Beams

by

Brian Weber, California Polytechnic State University, San Luis Obispo, CA

Damian Kachlakev, California Polytechnic State University, San Luis Obispo, CA

Simon Hettenkofer, Munich University of Applied Science, Munich, Germany

High Temperature Durability of CFRP Laminated RC Beams

This paper presents experimental results on the behavior of steel reinforced concrete beams strengthened with fiber-reinforced polymer (FRP) laminates at elevated temperatures. This unique study into the high temperature durability of this retrofit option focuses on beams simultaneously loaded while being subjected to thermal environments above the CFRP resin's glass transition temperature. The study consists of 17 identical flexurally reinforced beams proof tested at 20, 40, and 60 percent of the ultimate service load while maintaining FRP temperatures constant at 25°C, 75°C, 115°C, and 150°C.

A newly developed strain gauge specifically designed for integration into FRP laminates was used to measure the performance of the FRP reinforcement and the underlying concrete. During the laminate application process, strain gauges were embedded between two CFRP layers and on the concrete at the composite reinforcement interface. Rigid "pins" normal to the gauge plane, allow for simple electrical circuit completion outside of the cured composite without disturbing its mechanical properties. Strains were recorded in the composite as well as on the rebar, allowing for better characterization of the strengthened concrete beam. Strains and deflections were recorded for 4 hours allowing for comparison to standardized fire rating tests and applicable models. The results of the study suggested very good correlation between developed strains and deflections in the test beams

relative to the applied loads and temperatures. The engagement of the CFRP laminates in the load carrying beams' mechanisms, their ultimate strains and changing response at elevated temperatures with respect to time were of particular interest.

Introduction

In order for fiber reinforced polymer (FRP) laminates to become fully accepted as a reliable retrofit option, extensive studies need to be carried out to determine their durability at elevated temperatures. Despite the material's growing popularity and increasing use, there has been very little research done on the material's resistance to heat. The limited research available on the subject has focused primarily on testing FRP strengthened columns with additional fire coating products (Bisby, 2005) or concrete structures reinforced with FRP rebar (Saafi, 2002). Bisby's research shows that the insulation of FRP limits the temperatures reached in the composite to around 100°C, but still beyond the glass transition temperature of the epoxies used. For this reason, tests were carried out on CFRP strengthened beams without any of the additional coatings commercially available designed to increase the fire rating.

Beyond the glass transition temperature, T_g , the elastic modulus of a polymer is significantly reduced due to changes in its molecular structure. The value of T_g depends on the type of resin but is normally in the region of 60 to 82°C (140 to 180°F). In an FRP composite material, the fibers, which exhibit better thermal properties than the resin, can continue to support some load in the longitudinal direction until the temperature threshold of the fibers is reached. This can occur at temperatures near 1000°C (1800°F) for glass fibers and 260°C (500°F) for carbon. Due to a reduction in the force transfer between fibers through the bond to the resin, the tensile properties of the overall composite are reduced. Test results have indicated that temperatures of 260°C (500°F), much higher than the resin T_g , will reduce the tensile strength of GFRP and CFRP materials in excess of 20 percent (Gibson, 2004). Other properties affected by the shear transfer through the resin, such as bending strength, are reduced significantly at lower temperatures.

For bond critical applications of FRP systems, the properties of the polymer at the fiber-concrete interface are essential in maintaining bond between FRP and concrete. The structural role of the matrix, which is to hold the reinforcing fibers in place and transfer stresses from the concrete to the fibers, may be compromised as the temperature of the composite approaches the glass transition temperature of the polymer. The result is that the composite loses its tensile strength and stiffness. The failure of the composite occurs when the temperature of the fibers themselves reach the level at which they start

to degrade. The tensile strength of CFRP however, decreases consistently with increases in the temperature. The modulus of elasticity is relatively constant up to 100°C, and then decreases linearly with increases in temperature.

In applications where the performance of the FRP is dependent on the bond, extensive studies are needed to determine the performance of the epoxy at high temperatures.

The objectives of this paper are as follows:

- To investigate the flexural performance of RC beams strengthened with CFRP at high temperatures; to determine the changes in deflection as a result of temperature;
- To study the engagement mechanisms of CFRP laminates at elevated temperatures; and
- To analyze the development of strain in the FRP in relation to the strain developed in the reinforcing steel and concrete; and report the response characteristics at elevated temperatures with respect to time.

Research Significance

Concrete is widely accepted as a material capable of insulating rebar to withstand the extreme temperatures imposed during a fire. External reinforcement lacks this insulation and is therefore thermally vulnerable to the damaging effects of fire. Despite the growing popularity and increased use of fiber reinforced polymers for external strengthening, there has been limited research done on the materials resistance to heat when applied to concrete. The limited data available on this heat resistance should be alarming. This research is of paramount importance because it leads to a more rigorous approach in the development of safer and more qualified design guidelines.

Experimental Investigation

This investigation involved tests performed on 17 scaled rectangular concrete beams. All beams were identically strengthened with 2 layers of CFRP in flexural reinforcement and 1 layer of GFRP to enhance the shear capacity. Due to restrictions in geometry of the tested beams, internal steel stirrups were not feasible. The performance of the glass composite used in shear was not evaluated, and was considered to be unaffected by the application of heat. Each test was performed at a different temperature and load level, as shown in Table 1.

Description of Specimens

The rectangular beams had a length of 1219 mm (48 in), width of 127 mm (5 in), and height of 254 mm (10 in), as shown in Fig. 1. The longitudinal reinforcement consisted of two number 4 deformed steel bars with a diameter of 12.7 mm (0.5 in), area of 129 mm² (0.2 in²), and a depth of 222 mm (8.75 in). No internal steel stirrups were used. A 19 mm (0.75 in) radius on the longitudinal edges was created after the beams cured. This eased the high stress concentration in the U-shaped GFRP shear reinforcement at those locations.

The carbon composite material used for flexural reinforcement was a unidirectional fiber fabric. All beams were identically reinforced with two 1.0 mm (0.04 in) thick by 102 mm (4 in) wide layers. The glass composite material used for shear reinforcement was a bidirectional fiber fabric. The thickness of the GFRP used was 0.864 mm (0.034 in). The material properties for both types of FRP used is shown in Table 3.

Materials

A commercially available concrete was used in the construction of the specimens. Standard compression tests on 102 mm by 104 mm control cylinders revealed a 28-day concrete compressive strength of 23.4 MPa (3400 psi) on average following ASTM C39. Table 2 provides the mechanical properties of the reinforcing steel used. The CFRP fabric was bonded to the beam surface with an adhesive made of a resin and a hardener, both of which are specifically engineered for structural applications. Table 4 provides the mechanical and elastic properties of the resin epoxy used. The glass transition temperature is given with both the as-tested value and the value provided by the manufacturer. Determination of T_g was accomplished through the use of a carefully calibrated differential scanning calorimeter (DSC). Tests were repeated with a wide range of results on the same sample, confirming that the value of T_g is better represented by a range rather than a hard-set temperature. For the simplicity of discussion in this paper, the average of these tests is presented.

Test Setup

A unique oven chamber was developed for these tests which allowed for the beams to be loaded while also being heated. The chamber was constructed in a way that allowed the beam to be setup similar to a normal flexure test on the compression machine used. After setup was complete, the oven was installed around the specimen. Heat was supplied by two 3000 watt electric elements under the specimen's tension side. The oven is shown in Fig. 2. The beams were tested in three-point load flexure. This type of loading was chosen as it allowed for the use of the oven to heat the beams. All

beams were brought to the desired temperature prior to the start of the load. After reaching the maximum load desired for the test, the load was maintained for 4 hours.

Instrumentation

A carefully engineered set of instrumentation sensors were utilized to ensure satisfactory results even in the harsh high temperature conditions experienced in these tests. New strain gauges, designed specifically for integration into FRP laminates, were applied at the midspan of each specimen. Equipped with rigid “pins” soldered normal to the gauge plane, these gauges allowed for simple electrical circuit completion outside of the cured composite, leaving the composite’s mechanical properties undisturbed. The pins of the new gauges were pierced through the dry carbon fabric prior to saturation from the resin. Fig. 3a shows the pins that ease integration in the application process. Strains were recorded from two different length gauges, as seen in Fig. 3b. This paper will discuss the results produced from the shorter of the two gauges. In order to minimize the errors associated with thermal strains and specimen expansions, a modified quarter bridge circuit with an unstressed but heated “dummy” gauge was used. In addition, the load was not applied until after the beam reached its maximum temperature. Any variations in temperature would not significantly affect the strain signal output. Strains were recorded in the composite and on the concrete independently, allowing for better characterization of the FRP reinforced concrete member.

In addition to measuring the strain in the FRP, strains were recorded in the longitudinal steel rebar from gauges applied at the midspan of the beam. Deflections were recorded using multiple LVDTs; one at the midspan and one on the specimen above each of the end supports. This accounted for any settling of the FRP under the supports. Simple subtraction of these measurements produced the deflections presented in this paper. Temperatures were recorded using thermocouples embedded in each beam at key locations. The temperature of the reinforcing steel, the concrete-FRP interface, and between the individual layers within the FRP as well as 3 locations on the FRP surface were all recorded. The ambient oven air temperature was recorded by three thermocouples within the chamber to ensure thermal equilibrium between various locations.

Testing and Recording

The load was applied using a 1335 kN (300,000 lb) capacity universal Satec press. All loads were applied at a constant 5.3 kN/min (1200 lbs/min) rate. The signals from the Satec, strain gauges, thermocouples, and LVDTs were captured and monitored using an automatic data acquisition system from National Instruments. All data channels were sampled and

recorded at 1 Hz for the entire duration of the test. The temperature of the oven was controlled manually, aided by the use of a differential thermostat similar to those found in ordinary household ovens. The use of this thermostat resulted in the temperature within the oven cycling by 10°C (15°F). The maximum temperature recorded in the FRP was the temperature desired by the individual test.

Analysis of Results

The results from this experiment are provided in terms of temperature at the tested load levels representing 20, 40 and 60 percent of the ultimate strength, F_{ult} , of the strengthened beam. Tests were conducted for 4 hours or until flexural failure of the specimen. Of the beams that failed during testing, all failed as a result of yielding of the longitudinal steel in the maximum moment zone. Following the yielding of the steel, the flexural CFRP reinforcement completely debonded from the concrete substrate. Fig. 4 shows a typical beam after debonding under a support. A typical failure by yielding of the steel seen in this experiment is shown in Fig. 5. Following the failure, the steel strain-hardened, and continued to hold the load, despite the loss of the CFRP. Specimens N10, N11, N12, O4, and O5 all experienced similar failures.

A majority of the beams tested at the highest temperatures exhibited some form of epoxy degradation. The brownish discoloration was not uniform across the specimen, but rather was seen only in small patches of browns and yellows about 2 or 3 inches in diameter. The glass shear reinforcement took on a uniform dark burnt-yellow color, but remained intact until after the beam failed in flexure. Following the failure of a beam, careful examination of the heated composite revealed that both the CFRP and GFRP were exceedingly soft and pliable. Once cooled, the composite returned to its characteristically rigid nature.

Determination of the ultimate strength for the beams was performed at room temperature. The design load for the unstrengthened concrete beam was 79.8 kN (17,950 lb), but sustained 92 kN (20,700 lb) before the steel yielded during testing. After the application of two layers of CFRP, an identical beam (N1) held 176 kN (39,600 lb) prior to fiber rupture within the CFRP. This strengthening provided an impressive 91 percent increase in flexural capacity. The ultimate service load, F_{ult} , used in this research was 178 kN (40,000 lb). The ultimate elongation experienced by the FRP reinforcement was 1.1 percent, which is lower than the typical test value provided by the manufacturer.

Deflection Analysis

The results obtained from the midspan deflection measurements suggest a close correlation with

temperature. Fig. 6 through Fig. 8 present the deflection curves for tests loaded to 20, 40, and 60 percent of the ultimate load, respectively. All load levels clearly show an increase in deflection as a result of increases in the amount of heat applied. In addition to the changes in the deflection immediately following the load application, the deflection with respect to time is also presented. The room temperature deflection values observed in this test were consistent with those predicted prior to the experiment.

Fig. 6 shows the curves representing the deflection with respect to time for the specimens loaded to 20 percent of their ultimate strength. At this load level, the deflection increases by 12.1, 25.7, and 37.9 percent at 75°C, 115°C, and 150°C respectively in relation to room temperature deflections. These are the increases at the point immediately following the completion of the load application. This figure also shows that as the temperature of the FRP increases, the beam stiffness decreases. The room temperature test, N2T4, shows a 10.0 percent increase in deflection through the course of the four hour test. In contrast, the test at the same load level but at 150°C, N3, shows a large increase of almost 50 percent. This trend remains consistent through all other temperature levels. The beams tested at the 75°C and 115°C temperatures show a resonant pattern in the recorded deflection. This resonance can be disregarded as it is not related to load or deflection, but rather thermal expansions within the LVDT. As the temperature inside the oven mildly fluctuated, the small expansions and contractions of the center pin were recorded as a result of the heating element. This apparent measurement error was compensated for in subsequent tests through better insulating techniques.

The pattern seen in the lower load level is also shown in Fig. 7 at the 40 percent load level. The increases are more pronounced and defined at this higher load level though. In relation to the room temperature deflection, increases of 12.1, 25.7, and 37.9 percent at 75°C, 115°C, and 150°C respectively were observed. Once again, the room temperature test demonstrated a similar deflection increase of 10.3 percent while the higher 150°C beam, N7, shows a 35.3 percent gain. The changes over the 4 hour test were less pronounced however. This could be due to a relaxation of the FRP bond as the load is applied, as seen in the CFRP strain results in Fig. 10. FRP at higher temperatures is not capable of sustaining the loads demonstrated by the lower temperature capacities without a dramatic influence on the deflection.

The results from the highest load level are much more difficult to present as the two highest temperature tests failed prior to holding the load for the desired 4 hours. Fig. 8 presents the deflection curves for the 60 percent load level tests. Typical deflections were observed similar to those of the lower load tests with

respect to temperature. While these increases were not as dramatic as those in Fig. 6 and Fig. 7, they were still present, further suggesting the influence of temperature on bond between FRP and concrete even at the lower temperatures presented in this paper. Increases of 7.7, 16.5, and 25.9 percent at 75°C, 115°C, and 150°C respectively were recorded in relation to room temperature tests. Up to the failure of two highest temperature tests, the results are consistent with the other load levels in the demonstration that higher temperatures reduce the stiffness of strengthened beams.

Strains Analysis

This part of the study investigates the behavior of the CFRP and the steel rebar. Given the applied loads, the strain in the FRP was substantially greater in the specimens at room temperature than those at high temperatures. Conversely, the strain in the longitudinal steel rebar is greater in the specimens tested at the higher temperatures. Fig. 9 through Fig. 14 show these characteristics. It must be realized that all the recorded data was subjected to careful examination, analysis, and comparisons. For obvious reasons, however, it is not possible to report all the findings in this paper.

CFRP strain – Fig. 9 through Fig. 11 present the findings of the strain analysis in the composite. It should be noted that the strain analyzed was the strain developed in the flexural reinforcement only and not the glass fibers applied for shear enhancement. For all of the tests performed at room temperature, two distinct zones can be seen. These two zones are defined by the force required in the concrete to reach cracked section. The value of this force is seen in the rebar strain data as a decrease in stiffness. The corresponding FRP strain at that point should also reveal a new stiffness, assuming that the bond is fully adequate to support the load. In the room temperature tests that reached cracked section, N5 for example, this relationship is clearly seen. Increases in temperature demonstrated that the bond was increasingly insufficient to support and transfer the load from the concrete to the carbon fibers.

Fig. 9 illustrates the curves representing the strain with respect to load for the specimens loaded to 20 percent of their ultimate service load. At this load level, the strain decreases by -25.2, +76.6, and -64.3 percent at 75°C, 115°C, and 150°C respectively in relation to room temperature strains directly after reaching the maximum load of the test. The strain decreases as a result of an increase in FRP temperature. Localized debonding under the strain gauge is likely the cause of the uncharacteristically high strain level in beam N4. Even though this phenomenon cannot be seen in the figure, when looking at the strain level versus time for this specimen, the strain level decreased after sustaining the load for 15 minutes to a lower, more reasonable level in agreement with the rest of the tests.

The strain values in Fig. 10 show that at higher loads, the strain continues to decrease with changes in temperature. Decreases of -35.3, -21.6, and -53.6 percent were observed for the tests run at 75°C, 115°C, and 150°C respectively. With the heated FRP strain registering half of the room temperature strain, the shifted load must then be carried by the steel rebar, resulting in a beam with reduced capacity. The strain reversal of the beams tested at 75°C and 115°C in Fig. 10 and Fig. 11, as compared to their expected order, may be attributed to bond interactions on a micro scale. The epoxy used in the application of FRP to concrete must transfer stresses at two interface locations, from the concrete to the epoxy and again from the epoxy to the fibers. For composites loaded below the glass transition temperature, the majority of the material movement and resulting strain occurs between the fibers and the epoxy as the fibers align themselves parallel to the flexural load axis of the beam. As discussed earlier in this paper, the glass transition temperature should be considered a range of temperatures (not to be confused with a linear gradation) at which the epoxy cross-linking begins to relax. As the temperature is increased closer to the glass transition temperature range, the alignment of the fibers becomes easier, and better alignment is possible as shown in the strain curves. These small increases in temperature do not jeopardize the concrete-epoxy bond, but only the bond in small areas around the fibers. However, a composite loaded above its glass transition temperature range could experience slippage of the bond at the concrete-composite interface in addition to the small movements relating to fiber alignment, as seen in tests N10, N11, N12, O4, and O5. At lower temperatures the epoxy is stiffer, locking into the porous surface of the concrete. With the decreased shear strength of the FRP above the glass transition temperature, the concrete-epoxy bond relaxes and the phenomenon becomes much more pronounced. This slippage should be considered a classical definition of bond failure, resulting in possible structural collapse.

Careful examination of Fig. 10 reveals some hard to explain reversal of strain in specimen N6 near the beginning of the test, which might be explained by small movements in the specimen or other uncontrolled phenomenon. Should this be ignored and compensated, the data presented in the figure will show a steady increase of FRP strain inversely proportional to the increase of temperature.

For the highest load level tested, the FRP strains followed trends similar to those previously discussed. The strain decreases by -52.0, -30.2, and -59.6 percent at 75°C, 115°C, and 150°C respectively in relation to room temperature strains. This further shows that the application of higher temperatures reduces the flexural capacity of strengthened beams. When the load produced strains exceeding 50 percent of the strain

registered at room temperature, the assumption that plane sections remain plane becomes violated, most likely due to slippage of the bond between the FRP and concrete.

When reviewing the results in Fig. 9 through Fig. 11, one should also consider the small but possible effect caused by the thermal strain output not compensated for in the use of unstressed “dummy” gauges as discussed earlier in the paper. As the temperature increases, the strain reading slightly increased as well by about 50 microstrains in an unstressed specimen. Perfect temperature compensation would result in a relatively flat, stable output. Due to a host of variables, including material variations within the gauges themselves, the strain data should be considered as a very good approximation of the actual strain.

Steel reinforcement strain – The steel reinforcement strain was recorded by gauges on both segments of reinforcement at the section of maximum moment. Results indicate that the two individual strain channels are comparable, but for simplicity on the graphs presented, an average of the two is shown. At the lower load, the steel strain levels correlate with the temperature applied. Fig. 12 describes the average rebar strain at the 20 percent load level. As clearly shown, the trends presented by this paper remain consistent: higher temperatures reduce stiffness. The strain increases by 31.8, 58.3, and 78.9 percent at 75°C, 115°C, and 150°C respectively in relation to room temperature strains. Rebar stressed at the 40 percent load level increases by 63.2, 59.4, and 94.9 percent at 75°C, 115°C, and 150°C respectively. These results are presented in Fig. 13.

With the higher load levels combined with higher applied temperatures, the reinforcing steel yields prior to the target load being reached (Fig. 14). The behavior of the specimens heated to 115°C and 150°C at different load levels is difficult to compare. The results clearly indicate that at higher load levels combined with higher temperatures, the bond between the FRP and the concrete is compromised. The loss of this bond leaves the beam vulnerable to collapse if the load is sustained for a sufficient time. This accounts for the increases in the midspan deflection with respect to temperature. Thus, both FRP and rebar strain channels are comparable with each other, demonstrating the validity of the data presented.

The beams loaded to the highest level in this test, failed due to yielding of the steel at approximately 2200 microstrains. These failures are consistent with the load limitations suggested by ACI committee 440 equation 8-1.

$$(\phi R_n)_{\text{existing}} \geq (1.2S_{DL} + 0.85S_{LL})_{\text{new}} \quad (1)$$

This limit restricts the dependence on FRP during a fire as the existing structure must be able to resist a reasonable amount of load through the loss of the FRP strengthening system. The committee recommends that the existing strength of the structure be sufficient to resist the loads presented in Equation (1). The highest load selected in this study exceeded this limitation. Assuming that 15 percent of the applied force is considered a dead load, the right hand side of the equation limits the applied load to 80 kN (18,000 lb) for this research. Testing demonstrated capacities of 103.6 kN and 93.8 kN for beams at 115°C and 150°C, respectively, suggesting that this limitation is appropriately conservative.

Due to the failure of the high temperature and high load specimens, ultimate strain comparisons to the lower temperature results are not applicable. As presented in Fig. 14, the strains leading up to these failures are consistent with prior tests. Strains are reflective of the applied temperatures. The reduction in mechanical properties of steel due to high temperature remains unaffected until about 400°C (Saafi). After this point, any increase in temperature reduces these properties linearly. This experiment tested beams at elevated temperatures, below this threshold, and therefore assumes the properties remain constant for these lower temperature tests.

Conclusions

This study investigated the behavior of steel reinforced concrete beams with additional CFRP flexural reinforcement. Reductions in the performance of the beams were presented in terms of percentage compared to tests carried out at room temperature. Through the beam tests carried out, the authors were able to formulate some very interesting conclusions regarding the behavior of structures at elevated temperatures.

Based on the research, the following observations and conclusions were made:

- The effects on the performance of beams by elevating the temperature of externally bonded FRP are significant, even at small increases below the glass transition temperature;
- Above the glass transition temperature of the epoxy, the bond of the FRP to the concrete is not sufficient to resist the design loads in order to prevent failure. As a result, the strengthened system exhibits reduced stiffness, producing higher deflections; thus shifting the load demands to the reinforcing steel. Yielding of the steel was the common mode of failure in specimens tested at 115°C, and 150°C with 60 percent of the ultimate service load applied;
- The strengthening limitations of ACI committee 440

are sufficiently conservative and strict adherence to this must be followed on structures subjected to high temperatures; and

- The flexural capacities of CFRP strengthened beams were reduced by 40 and 46 percent at 115°C, and 150°C respectively. Reductions of this magnitude are significant. This research suggests that the temperature vulnerability of FRP is a major drawback and should be understood sufficiently before widespread use of FRP in high temperature environments continues.

Acknowledgements

The experimental work described in this paper was carried out at California Polytechnic State University, San Luis Obispo (Cal Poly). The technical assistance and cooperation of Simon Hettenkofer is acknowledged. The generous donation of composite materials by Fyfe Co., LLC is gratefully acknowledged. Similarly, the authors would like to recognize the donation of the newly developed strain gauges by the German company Hottinger Baldwin Measurement (HBM).

References

- ACI Committee 216, 1994, "Guide for Determining the Fire Endurance of Concrete Elements (216R-89)," American Concrete Institute, Farmington Hills, Mich., 48pp.
- ACI Committee 440, 2002, "Design and Construction of Externally Bonded FRP Systems for Strengthening Concrete Structures (440.2R-02)," American Concrete Institute, Farmington Hills, Mich., 45pp.
- Bisby, L.A.; Green, M.F.; Kodur, V.K.R., 2005, "Modeling the Behavior of Fiber Reinforced Polymer-Confined Concrete Columns Exposed to Fire," *Journal of Composites for Construction*, V. 9, No. 1, Jan.-Feb., pp. 15-24.
- Gibson, A.G.; Wright, P.N.H.; Wu, Y.S.; Mouritz, A.P.; Mathys, Z.; Gardiner, C.P., 2004, "The Integrity of Polymer Composites During and After Fire," *Journal of Composite Materials*, V. 38, No. 15, pp. 1283-1307.
- Saafi, M., 2002, "Effect of fire on FRP reinforced concrete members," *Composite Structures*, V. 58, No. 11-20.
- Weber, B., 2006, "High Temperature Durability of FRP Reinforced Concrete Beams," Master's thesis, Civil and Environmental Engineering Department, California Polytechnic State University, San Luis Obispo, Ca.

About the Authors

Brian Weber is a Civil Engineering graduate student at Cal Poly, San Luis Obispo focusing on composites in the Civil Engineering field. This paper summarizes his research efforts that concluded in September 2006.

Damian Kachlakev, PhD., PE, is an associate professor in the Department of Civil and Environmental Engineering at Cal Poly, SLO. He serves as a member of the ACI Committee 440- Fiber Reinforced Polymers, and ASTM D20.18.01- FRP for Concrete Reinforcement.

Simon Hettenkofer is a graduate of the Munich University of Applied Science in Munich, Germany.

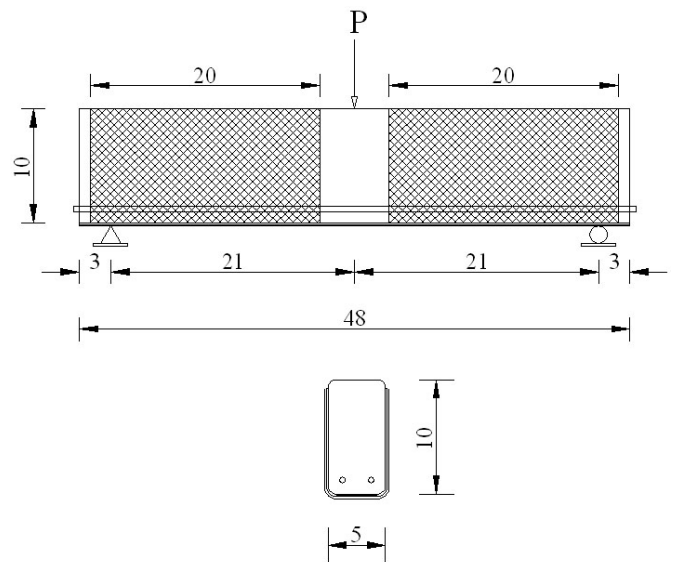


Figure 1 – Test setup and typical dimensions: (a) elevation; (b) cross section showing shear and flexure reinforcement. All dimensions in inches.



Figure 2 – Oven setup on press

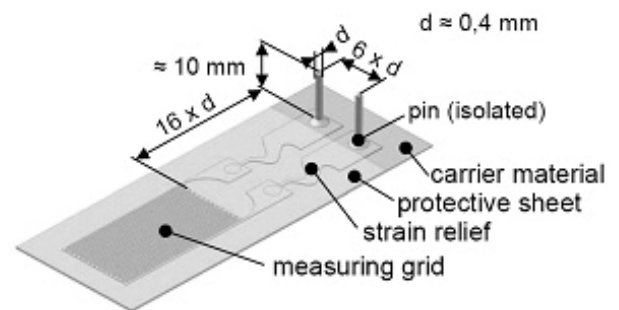


Figure 3a – Strain gauge construction

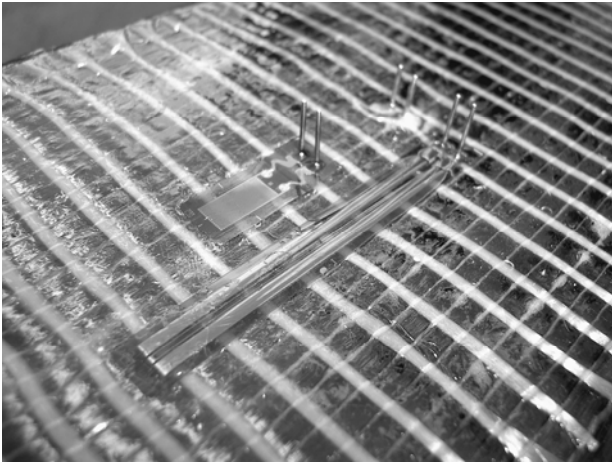


Figure 3b – Gauges to be integrated between FRP layers

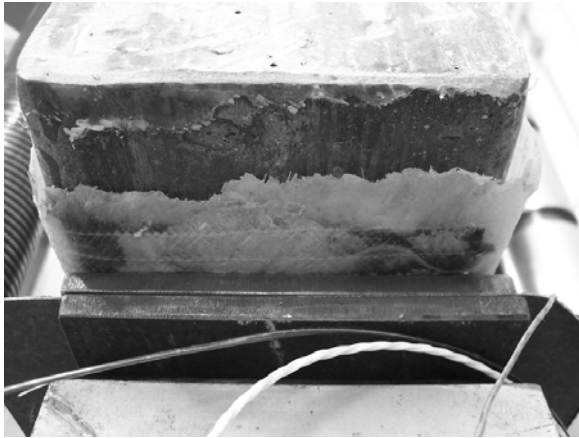


Figure 4 – Typical bond failure at support ends



Figure 5 – Typical failure in flexure

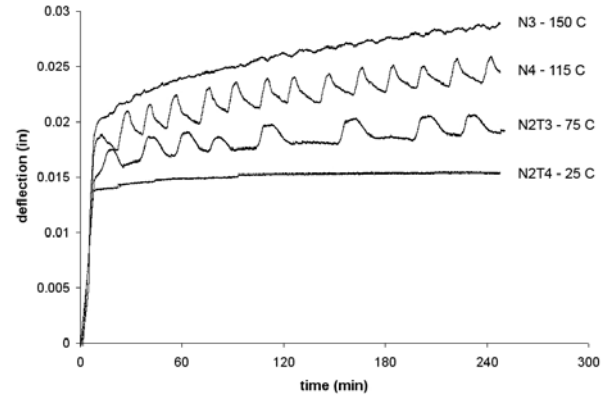


Figure 6 – Midspan deflection versus time in terms of temperature at 0.20 F_{ult} constant load

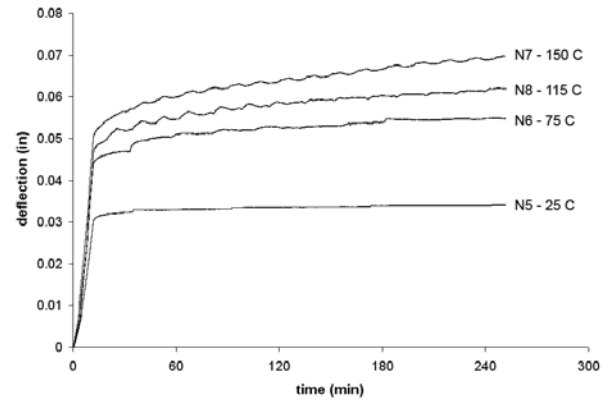


Figure 7 – Midspan deflection versus time in terms of temperature at 0.40 F_{ult} constant load

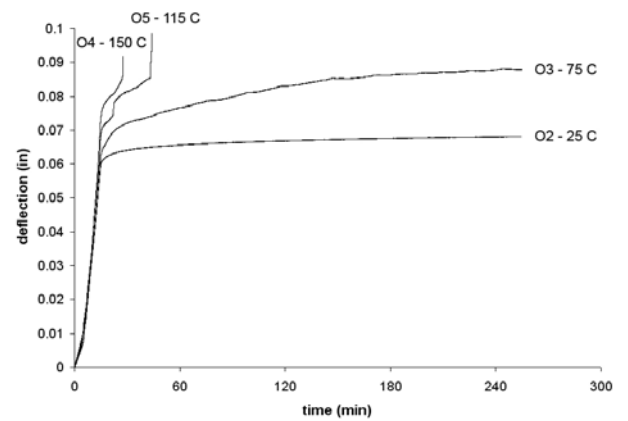


Figure 8 – Midspan deflection versus time in terms of temperature at 0.60 F_{ult} constant load

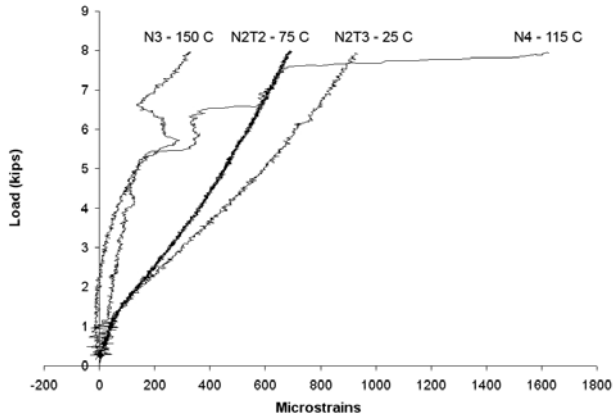


Figure 9 – FRP strain versus load in terms of temperature for $0.20 F_{ult}$ constant load

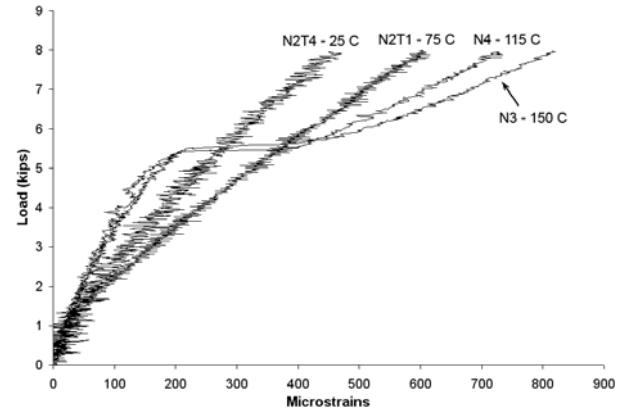


Figure 12 – Longitudinal steel strain versus load in terms of temperature for $0.20 F_{ult}$ constant load

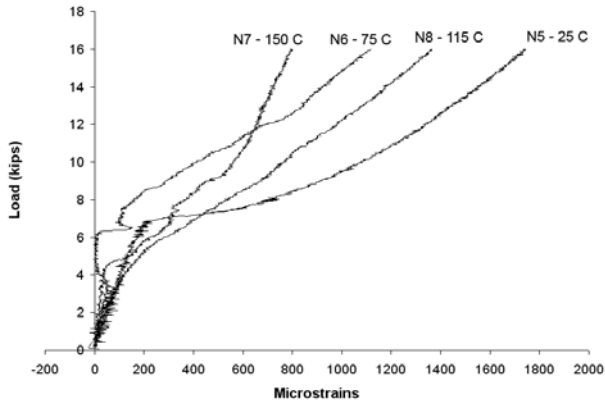


Figure 10 – FRP strain versus load in terms of temperature for $0.40 F_{ult}$ constant load

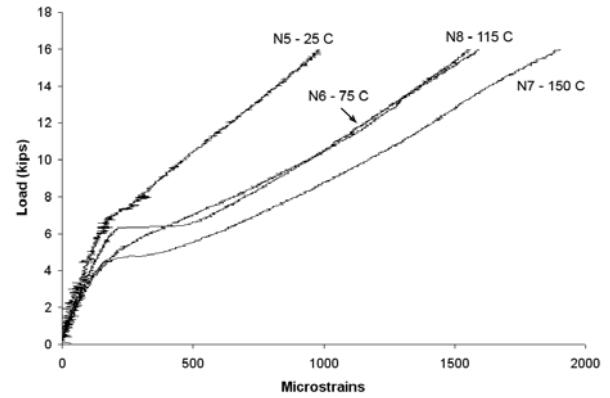


Figure 13 – Longitudinal steel strain versus load in terms of temperature for $0.40 F_{ult}$ constant load

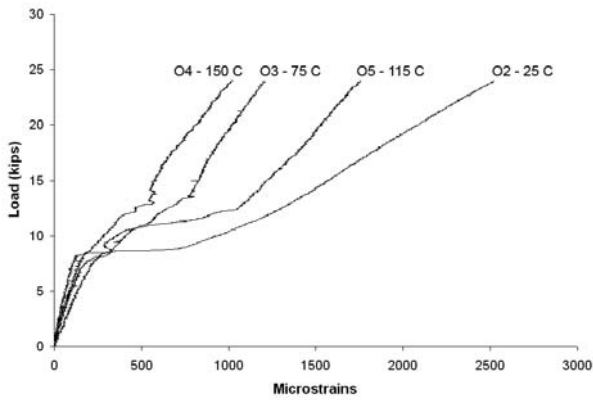


Figure 11 – FRP strain versus load in terms of temperature for $0.60 F_{ult}$ constant load

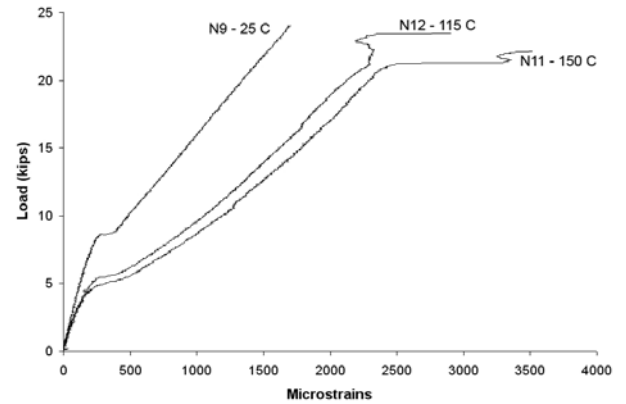


Figure 14. – Longitudinal steel strain versus load in terms of temperature for $0.60 F_{ult}$ constant load

		Temperature, °C			
		25 (75°F)	75 (170°F)	115 (235°F)	150 (300°F)
Load Level	0.20 F _{ult}	N2-T4	N2-T3	N4	N3
	0.40 F _{ult}	N5	N6	N8	N7
	0.60 F _{ult}	N9	N10	N12	N11
O2		O3	O5	O4	

Table 1 – Beam identification

Modulus of elasticity, GPa	200 (29.0 x 10 ⁶ psi)
Yield stress, MPa	420 (60.9 ksi)
Yield strain, microstrain	2100
Area, mm ²	129 (0.20 in ²)
Diameter, mm	12.7 (0.5 in)

Table 2 – Mechanical properties of steel reinforcement

Property	Carbon (one layer)	Glass (one layer)
	230	72.4
Modulus of elasticity, GPa	(33.4 x 10 ⁶ psi)	(10.5 x 10 ⁶ psi)
Ultimate elongation, %	1.7	4.5
Ultimate stress, GPa	3.79 (550 ksi)	3.24 (470 ksi)
Composite thickness, mm	1.0 (0.04 in)	0.864 (0.034 in)

Table 3 – Mechanical properties of CFRP and GFRP based on fibers alone

Glass transition temperature, °C	as provided by manufacturer	as tested
		82 (180°F)
Ultimate stress at 21°C, MPa	72.4 (10,500 psi)	
Modulus of elasticity, GPa	3.18 (461 x 10 ³ psi)	
Ultimate elongation, %	5.0	

Table 4 – Mechanical properties of epoxy